Competitive Nucleophilic Attack at CO and C$_\beta$ of the Allenyl Group in [Fe$_2$(CO)$_6$(μ-PPh$_2$)(μ-η^1:η^2-(H)C$_\alpha$=C$_\beta$=C$_\gamma$H$_2$)]. X-ray Crystal Structures of [Fe$_2$(CO)$_5$(μ-PPh$_2$)(μ-η^1(O):η^1(C):η^2(C)-{O=C(N^{t}BuH)CH$_2$}C=CH$_2$)]·0.5C$_6$H$_{14}$ and [Fe$_2$(CO)$_6$(μ-PPh$_2$)(μ-η^1:η^1-CH$_2$C(NCyH)CH$_2$]·MeCN

Simon Doherty,* Mark R. J. Elsegood, William Clegg, and Mark Waugh

Department of Chemistry, Bedson Building, The University of Newcastle upon Tyne, Newcastle upon Tyne, NE1 7RU, United Kingdom

Summary: The phosphido-bridged diiron allenyl complex [Fe$_2$(CO)$_6$(μ-PPh$_2$)(μ-η^1:$\eta^2_{\alpha,\beta}$-(H)C$_\alpha$=C$_\beta$=C$_\gamma$H$_2$)] **(1)** *reacts with primary amines to afford the amido-functionalized alkenyl complexes [Fe$_2$(CO)$_5$(μ-PPh$_2$)(μ-η^1(O): η^1(C):η^2(C)-{O=C(NRH)CH$_2$}C=CH$_2$)] (R = ^{t}Bu* **(2a)***, Ph* **(2b)***) via a novel coupling sequence involving a terminal carbonyl, the α-carbon of the allenyl, and a hydrogen migration step, as well as dimetallacyclopentanes [Fe$_2$(CO)$_6$(μ-PPh$_2$)(μ-η^1:η^1-CH$_2$C(NRH)CH$_2$] (R = ^{t}Bu* **(3a)***, Cy* **(3b)***) via nucleophilic attack at C$_\beta$.*

Although the first allenyl (−C(H)=C=CH$_2$) complexes were prepared over 25 years ago,[1] their synthesis and reactivity has received far less attention than other unsaturated hydrocarbyl ligands such as alkylidene (=CR^{1}R^2), alkylidyne (≡CR), vinylidene (=C=CR^{1}R^2), and acetylide (−C≡CR).[2] However, the past few years have witnessed an escalating interest in the chemistry of this cumulated hydrocarbyl fragment with the discovery of a broad-ranging reactivity that has heralded the beginning of a rich and diverse organometallic chemistry.[3] This recent resurgence of interest in the chemistry of transition-metal allenyl complexes has led to several landmark observations with a direct relevance to metal-mediated synthesis, including new allenyl bonding modes and ligand isomerization pathways as well as an extensive reactivity.[4−9] However, despite an intense research effort, the reactivity of the allenyl ligand has, until recently, been dominated by nucleophilic attack at C$_\beta$, although several reports now suggest that new reactivity patterns are beginning to emerge. Examples include a new reaction pathway for the μ-η^1:η^2-allenyl ligand in [Ru$_2$(CO)$_6$(μ-PPh$_2$)(μ-η^1:$\eta^2_{\beta,\gamma}$-(Ph)C=C=CPh$_2$)] involving displacement of the η^2-coordinated double bond by bis(diphenylphosphino)methane,[10] electrophilic attack at C$_\beta$ of the η^3-allenyl in [Pd$_2$(PPh$_3$)$_2$-(μ-Cl)(μ-η^3-(H)C=C=CH$_2$)],[11] and most recently, in our laboratory, an unprecedented regiospecific attack of phosphorus-based nucleophiles at C$_\alpha$ of the allenyl ligand in [Fe$_2$(CO)$_6$(μ-PPh$_2$)(μ-η^1:$\eta^2_{\alpha,\beta}$-(H)C=C=CH$_2$)] to generate new phosphino-substituted μ-η^1:η^2-alkenyl ligands.[12]

The binuclear complexes [M$_2$(CO)$_6$(μ-PPh$_2$)(μ-η^1:$\eta^2_{\beta,\gamma}$-(Ph)C=C=CH$_2$)] (M = Ru, Os) are prepared *via* the carbon-carbon coupling between CH$_2$N$_2$ and C$_\alpha$ of the acetylide in [M$_2$(CO)$_6$(μ-PPh$_2$)(μ-η^1:η^2-C≡CPh)];[3j] however, attempts to prepare their iron counterparts using a similar methodology have, to date, proven unsuccessful[13] and their chemistry remains unexplored. Recent studies in our laboratories have resulted in the isolation of [Fe$_2$(CO)$_6$(μ-PPh$_2$)(μ-η^1:$\eta^2_{\alpha,\beta}$-(H)C$_\alpha$=C$_\beta$=C$_\gamma$H$_2$)] **(1),** the first example of a phosphido-bridged diiron allenyl complex.[12] Although both [Ru$_2$(CO)$_6$(μ-PPh$_2$)(μ-η^1:$\eta^2_{\beta,\gamma}$-(Ph)C=C=CH$_2$)] and **1** contain μ-η^1:η^2-allenyl ligands, they differ structurally in that the C$_\beta$−C$_\gamma$ double bond is η^2-coordinated in the former while in **1** the allenyl ligand is coordinated via C$_\alpha$−C$_\beta$, the internal double bond. The successful preparation and isolation of **1**, in high yield, has provided us with an opportunity to compare the reactivity of μ-η^1:$\eta^2_{\alpha,\beta}$- and μ-η^1:$\eta^2_{\beta,\gamma}$-coordinated allenyl ligands. To this end, we have been exploring the reactivity of **1** with various nucleophiles and found the reaction products to depend markedly on the nature of the nucleophilic substrate. Herein we report the formation of the amido-functionalized alkenyl complexes

$^\otimes$ Abstract published in *Advance ACS Abstracts,* May 1, 1996.
(1) (a) Collman, J. P.; Cawse, J. N.; Kang, J. W. *Inorg. Chem.* **1968,** *12,* 2574. (b) Ariyarante, J. K. P.; Green, M. L. H. *J. Organomet. Chem.* **1963,** *1,* 90.
(2) (a) Bruce, M. I. *Chem. Rev.* **1991,** *91,* 197. (b) Holton, J.; Lappert, M. F.; Pearce, R.; Yarrow, P. I. W. *Chem. Rev.* **1983,** *83,* 135. (c) Mayr, A.; Hoffmeister, H. *Adv. Organomet. Chem.* **1991,** *32,* 27. (d) Schubert, U., Ed. *Advances in Metal Carbene Chemistry*; Kluwer Academic: Dordrecht, The Netherlands, 1989.
(3) For recent comprehensive reviews see: (a) Wojcicki, A. *New. J. Chem.* 1994, *18,* 61. (b) Doherty, S.; Corrigan, J. F.; Carty, A. J.; Sappa, E. *Adv. Organomet. Chem.* **1995,** *37,* 39. For Pd, Pt complexes: (c) Wouters, J. M. A.; Klein, R. A.; Elsevier, C. J.; Haming, L.; Stam, C. H. *Organometallics* **1994,** *13,* 4586. (d) Blosser, P. W.; Schimpff, D. G.; Gallucci, J. C.; Wojcicki, A. *Organometallics* **1993,** *12,* 1993. (e) Plantevin, V.; Blosser, P. W.; Gallucci, J. C.; Wojcicki, A. *Organometallics* **1994,** *13,* 3651. (f) Su, C.-C.; Chen, J.-T.; Lee, G.-H.; Wang, Y. *J. Am. Chem. Soc.* **1994,** *116,* 4999. For Pb complexes: (g) Seyferth, D.; Son, D. Y.; Shah, S. *Organometallics* **1994,** *13,* 2105. For binuclear complexes: (h) Nucciarone, D.; Taylor, N. J.; Carty, A. J. *Organometallics* **1986,** *5,* 1179. (i) Seyferth, D.; Womack, G. B.; Archer, C. M.; Dewan, J. C. *Organometallics* **1989,** *8,* 430. (j) Seyferth, D.; Archer, C. M.; Rushke, D. P.; Cowie, M.; Hilts, R. W. *Organometallics* **1991,** *10,* 3363.
(4) Huang, T.-M.; Hsu, R.-H.; Yang, C.-S.; Chen, J.-T.; Lee, G.-H.; Wang, Y. *Organometallics* **1994,** *13,* 3657.
(5) Breckenridge, S. M.; Taylor, N. J.; Carty, A. J. *Organometallics* **1991,** *10,* 837.

(6) Huang, T.-M.; Chen, J.-T.; Lee, G.-H.; Wang, Y. *J. Am. Chem. Soc.* **1993,** *115,* 1170.
(7) Wojcicki, A.; Shuchart, C. E. *Coord. Chem. Rev.* **1990,** *105,* 35.
(8) Ogoshi, S.; Fukunishi, Y.; Tsutsumi, K.; Kurosawa, H. *J. Chem. Soc., Chem. Commun.* **1995,** 2485.
(9) Carleton, N.; Corrigan, J. F.; Doherty, S.; Pixneur, R.; Sun, Y.; Taylor, N. J.; Carty, A. J. *Organometallics* **1994,** *13,* 4179.
(10) Blenkiron, P.; Corrigan, J. F.; Doherty, S.; Taylor, N. J.; Carty, A. J. Unpublished results.
(11) Ogoshi, S.; Tsutsumi, K.; Ooi, M.; Kurosawa, H. *J. Am. Chem. Soc.* **1995,** *117,* 10415.
(12) Doherty, S.; Elsegood, M. R. J.; Clegg, W.; Scanlan, T. H. *J. Chem. Soc., Chem. Commun.*, submitted for publication.
(13) Breckenridge, S. M.; MacLaughlin, S. A.; Taylor, N. J.; Carty, A. J. *J. Chem. Soc., Chem. Commun.* **1991,** 1718.

Scheme 1[a]
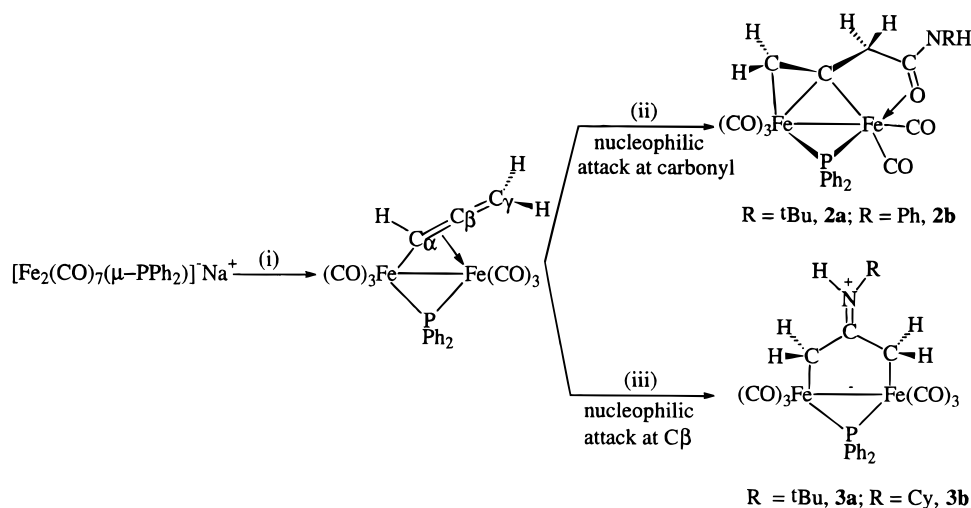
[a] Reagents and conditions: (i) BrCH$_2$C≡CH, Et$_2$O, room temperature; (ii) NRH$_2$ (R = ^{t}Bu, Ph), Et$_2$O, room temperature, (iii) NRH$_2$ (R = C$_6$H$_{11}$, ^{t}Bu), Et$_2$O, room temperature.

[Fe$_2$(CO)$_5$(μ-PPh$_2$)(μ-η^1(O):η^1(C):η^2(C)-{O=C(NHR)CH$_2$}-C=CH$_2$}] (R = ^{t}Bu (**2a**), Ph (**2b**)) and binuclear metallacycles [Fe$_2$(CO)$_6$(μ-PPh$_2$)(μ-η^1:η^1-CH$_2$C(NHR)CH$_2$] (R = ^{t}Bu (**3a**), Cy (**3b**)) that result from the competitive nucleophilic attack of RNH$_2$ (R = ^{t}Bu, Ph, Cy) at C$_\beta$ and the terminal carbonyl of **1**, respectively.

Solutions of **1** (0.150 g, 0.26 mmol) in diethyl ether react rapidly with *tert*-butylamine (0.015 mL, 0.26 mmol) over 5 h to afford two products, the deep red amido-functionalized alkenyl complex [Fe$_2$(CO)$_5$(μ-PPh$_2$)-(μ-η^1(O):η^1(C):η^2(C)-{O=C(NH^{t}Bu)CH$_2$}C=CH$_2$}] (**2a**) and the golden yellow dimetallacyclopentane [Fe$_2$(CO)$_6$(μ-PPh$_2$)(μ-η^1:η^1-CH$_2$C(N^{t}BuH)CH$_2$] (**3a**) in 65 and 10% yields respectively. In sharp contrast the reaction of **1** with aniline is highly regioselective, forming [Fe$_2$(CO)$_5$(μ-PPh$_2$)(μ-η^1(O):η^1(C):η^2(C)-{O=C(NHPh)CH$_2$}C=CH$_2$}] (**2b**) in 73% yield as the sole product after chromatographic workup and crystallization, while cyclohexylamine reacts at C$_\beta$ to afford golden yellow [Fe$_2$(CO)$_6$(μ-PPh$_2$)(μ-η^1:η^1-CH$_2$C(NCyH)CH$_2$] (**3b**) (69%) (Scheme 1).

Compounds **2a,b** and **3a,b** have been characterized by a combination of IR and ^{31}P{^{1}H}, ^{1}H, ^{1}H{^{31}P}, and (for **2a**) 2D ^{13}C–^{1}H correlated NMR spectroscopy, as well as mass spectrometry and elemental analysis.[14,15]

The ^{31}P{^{1}H} NMR spectra of compounds **2** and **3** are unexceptional, each containing resonances in the region characteristic of phosphido ligands bridging Fe–Fe bonds (δ 165–175 ppm). The ^{1}H NMR spectrum of **2a** contains four distinct allene resonances (δ 4.23, 3.18, 2.78, 2.21 ppm),[14] suggesting a substantial rearrangement of the bonding mode of this hydrocarbyl fragment. This conclusion was further reinforced by the disappearance of the two high-field ^{13}C allenyl resonances of **1** (δ(C$_\alpha$) **118.3**, δ(C$_\gamma$) **79.0** ppm) and the appearance of two low-field resonances (δ 183.1, 168.0 ppm) together with two additional signals at much higher field (δ 63.2, 57.9 ppm). A full spectroscopic assignment of the ^{1}H and ^{13}C NMR resonances of the bridging hydrocarbyl ligand in **2a** was accomplished using a combination of ^{1}H, ^{1}H{^{31}P} ^{1}H–^{1}H COSY, and ^{1}H–^{13}C heteronuclear single- and multiple-bond correlation studies together with a knowledge of the X-ray crystal structure (*vide infra*). The signals at δ 168.0 (C$_\beta$), 63.2 (C$_\gamma$), and 57.9 (C$_\alpha$) are derived from the allenyl ligand in **1**, while the remaining resonance at δ 183.1 ppm belongs to the amido carbonyl carbon generated during a novel amine–carbonyl–allenyl coupling sequence. These unusual spectroscopic features coupled with the amine-dependent regioselectivity prompted a single-crystal X-ray study of **2a**.0.5C$_6$H$_{14}$ (Figure 1).[16] The most remarkable feature of this structure is the transformation of the cumulated μ-η^1:η^2-allenyl hydrocarbon into an amido-functionalized μ-η^1:η^2-alkenyl ligand. The oxygen atom O(4) of the amido functionality coordinates to Fe(1), forming a five-membered oxametallacycle with an Fe–O bond length (Fe(1)–O(4) = 2.017(5) Å) similar to that

(14) Spectroscopic data for **2a** and **2b** are as follows. Compound **2a**: IR (ν(CO), C$_6$H$_{12}$, cm^{-1}) 2029 w, 1996 s, 1959 m, 1945 w, 1930 w, 1617 w; ^{31}P{^{1}H} NMR (101.3 MHz, CDCl$_3$, δ) 173.0 (s, μ-PPh$_2$) ppm; ^{13}C-{^{1}H} NMR (50.3 MHz, CDCl$_3$, δ) 218.7 (d, $^2J_{PC}$ = 12.0 Hz, CO), 215.7 (d, $^2J_{PC}$ = 3.0 Hz, CO), 213.5 (d, $^2J_{PC}$ = 15.0 Hz, CO), 183.1 (s, *C*(*O*)NH^{t}Bu), 168.0 (d, $^2J_{PC}$ = 27.0 Hz, CH$_2$=*C*CH$_2$C(*O*)), 125–140 (m, *C*$_6$H$_5$), 63.2 (d, $^2J_{PC}$ = 8.7 Hz, *C*H$_2$=CCH$_2$C(*O*)), 57.9 (d, $^3J_{PC}$ = 4.6 Hz, CH$_2$=C*C*H$_2$C(*O*)), 53.0 (s, C(*O*)*C*(CH$_3$)$_3$), 28.5 (s, C(*O*)C(*C*H$_3$)$_3$) ppm; ^{1}H NMR (200.13 MHz, CDCl$_3$, δ) 7.0–7.6 (m, C$_6$*H$_5$*, 10H), 5.80 (br s, N–*H*), 4.23 (br d, $^2J_{HH}$ = 19.1 Hz, 1H, C*H$_a$*H$_b$C(*O*)NH^{t}Bu), 3.18 (dd, $^3J_{PH}$ = 11.6 Hz, $^2J_{HH}$ = 2.6 Hz, 1H, C*H$_a$*H$_b$=C), 2.78 (dd, $^2J_{HH}$ = 19.1 Hz, $^4J_{PH}$ = 2.60 Hz, 1H, CH$_c$*H$_d$*C(*O*)NH^{t}Bu), 2.21 (br d, $^3J_{PH}$ = 7.0 Hz, 1H, C*H$_a$*H$_b$=C), 1.21 (s, 9H, NC(C*H$_3$*)$_3$) ppm; MS (*m/z*, 70 eV) 577 (M$^+$), 549 (M$^+$ – CO), 521 (M$^+$ – 2CO), 493 (M$^+$ – 3CO), 465 (M$^+$ – 4CO), 437 (M$^+$ – 5CO). Anal. Calcd for C$_{25}$H$_{24}$Fe$_2$NO$_6$P: C, 52.02; H, 4.19; N, 2.43. Found: C, 50.81; H, 3.65; N, 2.29. Compound **2b**: IR (ν(CO), C$_6$H$_{12}$, cm^{-1}) 2031 w, 1998 s, 1963 m, 1952 w, 1934 w; ^{31}P{^{1}H} NMR (101.3 MHz, CDCl$_3$, δ) 173.6 (s, μ-PPh$_2$) ppm; ^{13}C{^{1}H} NMR (50.3 MHz, CDCl$_3$, δ) 214.0 (d, $^2J_{PC}$ = 12.0 Hz, CO), 207.0 (d, $^2J_{PC}$ = 3.5 Hz, CO), 204.5 (d, $^2J_{PC}$ = 14.0 Hz, CO), 181.8 (s, *C*(*O*)NHPh), 168.0 (d, $^2J_{PC}$ = 27.0 Hz, CH$_2$=*C*CH$_2$C(*O*)), 120–144 (m, *C*$_6$H$_5$), 63.1 (d, $^2J_{PC}$ = 7.8 Hz, *C*H$_2$=CCH$_2$C(*O*)), 58.0 (s, CH$_2$=C*C*H$_2$C(*O*)) ppm; ^{1}H NMR (200.13 MHz, CDCl$_3$, δ) 8.0 (br s, N–*H*), 6.6–7.6 (m, 15H, C$_6$*H$_5$*), 4.28 (br d, $^2J_{HH}$ = 18.9 Hz, 1H, C*H$_c$*H$_d$C(*O*)NHPh), 3.16 (br d, $^2J_{PH}$ = 12.2 Hz, 1H, CH$_a$*H$_b$*=C), 3.01 (br d, $^2J_{HH}$ = 18.9 Hz, 1H, CH$_c$*H$_d$*C(*O*)NHPh), 2.20 (br d, $^2J_{HH}$ = 12.0 Hz, 1H, CH$_c$*H$_d$*=C).

(15) Selected data for **3a** and **3b** are as follows. Compound **3a**: IR (ν(CO), C$_6$H$_{12}$, cm^{-1}) 2046 m, 2003 s, 1976 m, 1957 m, 1942 w; ^{31}P-{^{1}H} NMR (101.3 MHz, CDCl$_3$, δ) 192.3 ppm; ^{13}C{^{1}H} NMR (50.3 MHz, CDCl$_3$, δ) 115.0 (br s, CO), 191.0 (s, C$_\beta$), 128–135 (m, *C*$_6$H$_5$), 48.0 (s, *C*(CH$_3$)$_3$), 30.5 (s, C(*C*H$_3$)$_3$), 30.0 (s, C$_\alpha$*H*$_2$C$_\gamma$*H*$_2$) ppm; ^{1}H NMR (200.13 MHz, CDCl$_3$, δ) 7.0–7.8 (m, C$_6$*H$_5$*, 10H), 5.3 (br s, N–*H*), 1.45 (s, CH$_2$, 4H), 1.31 (s, C(C*H$_3$*)$_3$, 9H). Compound **3b**: IR (ν(CO), C$_6$H$_{12}$, cm^{-1}) 2044 m, 2004 s, 1974 m, 1957 m, 1949 w; ^{31}P{^{1}H} NMR (101.3 MHz, CDCl$_3$, δ) 191.8 (s, μ-PPh$_2$) ppm; ^{1}H NMR (200.13 MHz, CDCl$_3$, δ) 7.1–7.9 (m, C$_6$*H$_5$*, 10H), 5.2 (br d, $^3J_{HH}$ = 8.2 Hz, N–*H*, 1H), 3.2 (m, N–C–*H*, 1H), 1.93 (s, CH$_2$, 4H), 0.7–1.7 (m, Cy–*H*$_2$, 10H); ^{13}C{^{1}H} NMR (50.3 MHz, CDCl$_3$, δ) 205.0 (br s, CO), 191.6 (s, C$_\beta$), 128–133 (m, *C*$_6$H$_5$), 52.6 (s, Cy–*C*–N), 33.8 (s, Cy–*C*H$_2$), 32.8 (s, Cy–*C'*H$_2$), 25.2 (s, Cy–*C''*H$_2$), 24.6 (d, C$_\alpha$*H*$_2$C$_\gamma$*H*$_2$, $^2J_{PC}$ = 4.0 Hz). Anal. Calcd for C$_{27}$H$_{26}$Fe$_2$NO$_6$P·C$_2$H$_3$N: C, 54.01; H, 4.54; N, 4.35. Found: C, 53.60; H, 4.32; N, 4.21.
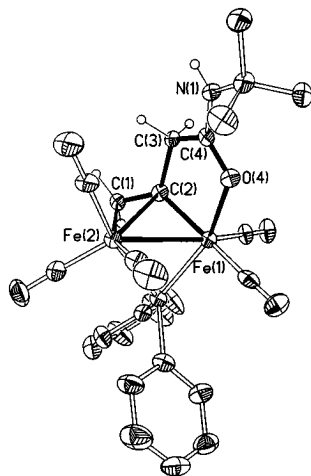
Figure 1. Molecular structure of $[Fe_2(CO)_5(\mu\text{-}PPh_2)(\mu\text{-}\eta^1(O):\eta^1(C):\eta^2(C)\text{-}\{O=C(N^tBuH)CH_2\}C=CH_2)]$ (**2a**) illustrating the $\mu\text{-}\eta^1:\eta^2$ coordination of the alkenyl ligand and highlighting the metallacyclic nature of the amido–carbonyl interaction with Fe(1). Ellipsoids are at 40% probability; ^{t}Bu and phenyl H atoms are omitted. Selected bond lengths (Å) and angles (deg) are as follows: Fe(1)–Fe(2) = 2.5952(14), Fe(1)–C(2) = 1.944(7), Fe(2)–C(2) = 2.124-(7), Fe(2)–C(1) = 2.180(7), Fe(1)–O(4) = 2.017(5), C(1)–C(2) = 1.393(10), C(2)–C(3) = 1.500(10), C(3)–C(4) = 1.501(10), C(4)–O(4) = 1.253(8); Fe(1)–O(4)–C(4) = 115.3-(4), C(1)–C(2)–C(3) = 118.8(6), C(2)–C(3)–C(4) = 109.4-(6), C(3)–C(4)–O(4) = 116.9(6).

recently reported by Hogarth in $[Fe_2(CO)_4\{C(CO_2\text{-}Me)=CHC(OMe)=O\}(\mu\text{-}PPh_2)(\mu\text{-}dppm)]$ (2.024(3) Å).[17] In **2a** the alkenyl group is σ-bonded to Fe(1) (Fe(1)–C(2) = 1.944(7) Å) and π-bonded to Fe(2) (Fe(2)–C(1) = 2.180(7) Å, Fe(2)–C(2) = 2.124(7) Å). The C(1)–C(2) bond length (1.393(10) Å) shows the expected increase upon coordination to a metal center and is comparable to values in other phosphido-bridged diiron alkenyl complexes.[18] The amido C–O bond (C(4)–O(4) = 1.253-(8) Å) is typical of a single bond in a five-membered oxametallacycle.[14] The formation of this hydrocarbyl ligand accounts for the two distinctive $\mu\text{-}\eta^1:\eta^2$-alkenyl resonances in the $^{13}C\{^1H\}$ NMR spectra of **2a** (δ 168.0, 63.2 ppm) and **2b** (δ 171.0, 65.4 ppm).[18] The alkenyl ligands in **2a,b** are derived from **1** by nucleophilic attack of amine at a terminal carbonyl group followed by regiospecific coupling of this functionality with C_α of the allenyl ligand and a "formal" 1,3-hydrogen migration. There is no precedent for the generation of an amido-functionalized $\mu\text{-}\eta^1:\eta^2$-alkenyl ligand via an amine–carbonyl–allenyl coupling sequence; however, a closely related coupling sequence has recently been used to
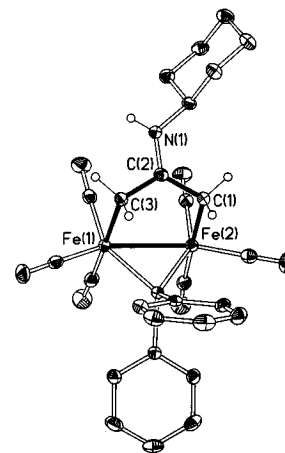
Figure 2. Molecular structure of $[Fe_2(CO)_6(\mu\text{-}PPh_2)(\mu\text{-}\eta^1:\eta^1\text{-}CH_2C(NCyH)CH_2]$ (**3b**) highlighting the C_3Fe_2 dimetallacycle. Ellipsoids are at 40% probability; phenyl and cyclohexyl H atoms are omitted. Selected bond lengths and angles (Å) are as follows: Fe(1)–Fe(2) = 2.7453(4), Fe(1)–C(3) = 2.118(2), Fe(2)–C(1) = 2.127(2), C(1)–C(2) = 1.441-(3), C(2)–C(3) = 1.461(3), C(2)–N(1) = 1.328(3); Fe(2)–Fe(1)–C(3) = 86.80(6), Fe(1)–Fe(2)–C(1) = 86.73(6), Fe(2)–C(1)–C(2) = 104.39(14), Fe(1)–C(3)–C(2) = 104.14(14), C(1)–C(2)–C(3) = 119.4(2).

prepare the amido- and carboxylate-functionalized η^3-allyl and η^1-alkenyl complexes $[Cp(CO)_2W\{\eta^3\text{-}CH_2CHCH\text{-}(CONHR)\}]$ (**5**) and $[Cp(CO)_2W[\eta^1\text{-}C(CH_3)=CHC(O)OR]$ (**6**) from $[CpW(CO)_2(\eta^1\text{-}CH=C=CH_2)]$ and RNH_2 and ROH, respectively.[19] Despite similarities, the formation of **2a,b** requires a "formal" hydrogen migration to C_α, while the generation of **5** and **6** necessitates migration of hydrogen to C_γ and C_β, respectively.

The $^{13}C\{^1H\}$ NMR spectra of **3a,b** both contain two distinct hydrocarbyl resonances (**3a**, $\delta(C_\beta)$ 191.0 δ-$(C_\alpha=C_\gamma)$ 30.0; **3b**, $\delta(C_\beta)$ 191.6, $\delta(C_\alpha=C_\gamma)$ 24.6 ppm), one of which is located at high field relative to those of the allenyl fragment in **1** (*vide supra*), indicating that this hydrocarbyl ligand has been modified. In fact, these ^{13}C NMR chemical shifts are in the region characteristic of the C_3 bridging ligand in the dimetallacyclopentane complexes $[Ru_2(CO)_6(\mu\text{-}PPh_2)(\mu\text{-}\eta^1:\eta^1CH_2\text{-}C(NRH)CH_2]$ (R = Et, Cy). Since ^{13}C NMR spectroscopy has proven to be an extremely reliable probe of structure and bonding in zwitterionic bridging hydrocarbyls,[20] we have been able to confidently formulate **3a,b** as the binuclear dimetallacylclopentane complexes $[Fe_2(CO)_6(\mu\text{-}PPh_2)(\mu\text{-}\eta^1:\eta^1\text{-}CH_2C(NRH)CH_2]$ (R = ^{t}Bu, Cy), an assignment which has been confirmed crystallographically (R = Cy (**3b**)).[21]

The molecular structure of **3b·MeCN** (Figure 2) confirms that cyclohexylamine reacts regiospecifically

(16) Crystal data for **2a**·0.5C_6H_{14}: $C_{28}H_{31}Fe_2NO_6P$, M_r = 620.6, monoclinic, $P2_1/c$, a = 10.1958(14) Å, b = 8.6428(12) Å, c = 33. 686(5) Å, β = 94.827(4)°, V = 2957.9(7) Å^3, Z = 4, D_{calcd} = 1.393 g cm^{-3}, μ = 1.075 mm^{-1} (Mo Kα, λ = 0.710 73 Å), $F(000)$ = 1284; 12 075 reflections (θ_{max} = 22.5°) measured on a Siemens SMART CCD area detector diffractometer at 160 K, 3859 unique data (R_{int} = 0.0787), semiempirical absorption correction (transmission 0.351–0.952 for crystal size 0.88 × 0.20 × 0.09 mm); structure solution by direct methods, refinement on F^2 with statistics-based weighting scheme, anisotropic displacement parameters and constrained isotropic H atoms; final wR2 = $\{\Sigma[w(F_o^2 - F_c^2)^2]/\Sigma[w(F_o^2)^2]\}^{1/2}$ = 0.2574 for all data, conventional R = 0.0944 on F values for 3243 reflections having $F_o^2 > 2\sigma(F_o^2)$, S = 1.226 on F^2 for all data and 346 refined parameters; final difference map extremes +2.01 and −1.43 e Å^{-3}, close to Fe atoms.
(17) (a) Hogarth, H.; Lavender, M. H. *J. Chem. Soc., Dalton Trans.* **1994**, 3389.
(18) MacLaughlin, S. A.; Doherty, S.; Taylor, N. J.; Carty, A. J. *Organometallics* **1992**, *11*, 4315.

(19) Tseng, T.-W.; Wu, I.-Y.; Tsai, J.-H.; Lin, Y.-C.; Cheng, D.-J.; Lee, G.-H.; Chen, M.-C.; Wang, Y. *Organometallics* **1994**, *13*, 3963.
(20) Cherkas, A. A.; Breckenridge, S. M.; Carty, A. J. *Polyhedron* **1992**, *11*, 107.
(21) Crystal data for **3b·MeCN**: $C_{29}H_{29}Fe_2N_2O_6P$, M_r = 644.2, orthorhombic, $P2_12_12_1$, a = 8.9423(9) Å, b = 16.884(2) Å, c = 19.763(2) Å, V = 2983.9(5) Å^3, Z = 4, D_{calcd} = 1.434 g cm^{-3}, μ = 1.069 mm^{-1}, $F(000)$ = 1328; 11 703 reflections measured (θ_{max} = 28.5°) at 160 K, 6853 unique data (R_{int} = 0.0360), transmission 0.666–0.797 for crystal size 0.39 × 0.24 × 0.04 mm; refinement as for **2a**·0.5C_6H_{14} except for freely refined N–H; wR2 = 0.0611 for all data, R = 0.0289 on F values for 6145 reflections having $F_o^2 > 2\sigma(F_o^2)$, S = 1.077 for 367 refined parameters; final difference map extremes +0.26 and −0.25 e Å^{-3}, racemic twinning indicated by absolute structure parameter of 0.560-(10) (Flack, H. D. *Acta Crystallogr., Sect. A* **1983**, *39*, 876).

at C_β in **1**, with proton transfer across the $C_\alpha=C_\beta$ double bond, to generate the zwitterionic dimetallacyclopentane $[Fe_2(CO)_6(\mu\text{-}PPh_2)(\mu\text{-}\eta^1:\eta^1\text{-}CH_2C(NCyH)CH_2]$. The short $N(1)-C(2)$ bond distance (1.328(3) Å) and planarity at $N(1)$ and $C(2)$ (sum of angles 359.6 and 359.9°, respectively) confirms that **3b** has substantial imine character. The carbon−carbon bond lengths within the metallacycle $(C(1)-C(2) = 1.441(3)$ Å, $C(2)-C(3) = 1.461(3)$ Å) are remarkably similar to those in its ruthenium counterpart $[Ru_2(CO)_6(\mu\text{-}PPh_2)(\mu\text{-}\eta^1:\eta^1\text{-}CPhHC(NEtH)\text{-}CH_2]$ and reflect their $C(sp^2)-C(sp^3)$ single-bond character.[5] The five-membered metallacycle adopts an envelope conformation in which the C_3 flap is *exo* with respect to the Fe_2P triangle and the $Fe(CO)_3$ units are eclipsed with respect to each other, presumably constrained by the rigid three-carbon hydrocarbyl bridging ligand. There is an H-bonding interaction between the MeCN of crystallization and NCy-*H*(1) $(N(2)-H(1) = 2.23$ Å, $N(2)-H(1)-N(1) = 174°)$.

The substrate-dependent regiospecific addition of amines at either a terminal carbonyl group or the β-carbon of the $\mu\text{-}\eta^1:\eta^2_{\alpha,\beta}$-coordinated allenyl in $[Fe_2(CO)_6(\mu\text{-}PPh_2)(\mu\text{-}\eta^1:\eta^2_{\alpha,\beta}\text{-}(H)C_\alpha=C_\beta=C_\gamma H_2)]$ contrasts sharply with the exclusive formation of metallacyclopentanes and pentenes via attack of nitrogen and phosphorus nucleophiles at C_β of the $\mu\text{-}\eta^1:\eta^2_{\beta,\gamma}$-allenyl ligand in $[Ru_2(CO)_6(\mu\text{-}PPh_2)(\mu\text{-}\eta^1:\eta^2_{\beta,\gamma}\text{-}(Ph)C=C=CH_2)]$. In fact, the reactivity of mononuclear η^3- and $\mu\text{-}\eta^1:\eta^2_{\beta,\gamma}$-allenyl ligands has been dominated by the electrophilic

nature of C_β and only recently have new reaction pathways been discovered. In summary, our studies have demonstrated a remarkable difference between the chemistry of $\mu\text{-}\eta^1:\eta^2_{\alpha,\beta}$- and $\mu\text{-}\eta^1:\eta^2_{\beta,\gamma}$-allenyl complexes of iron and ruthenium, respectively, and clearly this new reactivity pattern suggests a potential role for $\mu\text{-}\eta^1:\eta^2_{\alpha,\beta}$-allenyl complexes, as three-carbon transfer reagents, in metal-mediated synthesis. We are currently developing the chemistry of **1** and $[Fe_2(CO)_6(\mu\text{-}PPh_2)(\mu\text{-}\eta^1:\eta^2_{\alpha,\beta}\text{-}(Ph)C=C=CH_2]$ in order to establish the existence of a structure-reactivity relationship.

Supporting Information Available: For **2a**·0.5C_6H_{14} and **3b**·MeCN, details of the structure determination (Tables S1 and S6), non-hydrogen atomic positional parameters (Tables S2 and S7), bond distances and angles (Tables S3 and S8), anisotropic displacement parameters (Tables S4 and S9), and hydrogen atom coordinates (Tables S5 and S10) and spectroscopic data for **2a,b** and **3a,b** (Table S11) (14 pages). Ordering information is given on any current masthead page. Observed and calculated structure factor tables are available from the authors upon request.

OM960079+